

# The generation of neutrophils in the bone marrow is controlled by autophagy

S Rožman<sup>1</sup>, S Yousefi<sup>1</sup>, K Oberson<sup>1</sup>, T Kaufmann<sup>1</sup>, C Benarafa<sup>2</sup> and HU Simon<sup>\*1</sup>

Autophagy has been demonstrated to have an essential function in several cellular hematopoietic differentiation processes, for example, the differentiation of reticulocytes. To investigate the role of autophagy in neutrophil granulopoiesis, we studied neutrophils lacking *autophagy-related (Atg) 5*, a gene encoding a protein essential for autophagosome formation. Using Cre-recombinase mediated gene deletion, *Atg5*-deficient neutrophils showed no evidence of abnormalities in morphology, granule protein content, apoptosis regulation, migration, or effector functions. In such mice, however, we observed an increased proliferation rate in the neutrophil precursor cells of the bone marrow as well as an accelerated process of neutrophil differentiation, resulting in an accumulation of mature neutrophils in the bone marrow, blood, spleen, and lymph nodes. To directly study the role of autophagy in neutrophils, we employed an *in vitro* model of differentiating neutrophils that allowed modulating the levels of ATG5 expression, or, alternatively, intervening pharmacologically with autophagy-regulating drugs. We could show that autophagic activity correlated inversely with the rate of neutrophil differentiation. Moreover, pharmacological inhibition of p38 MAPK or mTORC1 induced autophagy in neutrophilic precursor cells and blocked their differentiation, suggesting that autophagy is negatively controlled by the p38 MAPK–mTORC1 signaling pathway. On the other hand, we obtained no evidence for an involvement of the PI3K-AKT or ERK1/2 signaling pathways in the regulation of neutrophil differentiation. Taken together, these findings show that, in contrast to erythropoiesis, autophagy is not essential for neutrophil granulopoiesis, having instead a negative impact on the generation of neutrophils. Thus, autophagy and differentiation exhibit a reciprocal regulation by the p38–mTORC1 axis.

*Cell Death and Differentiation* (2015) 22, 445–456; doi:10.1038/cdd.2014.169; published online 17 October 2014

Autophagy is an evolutionarily conserved mechanism, by which portions of cytoplasm are engulfed in a double-membrane structure, known as the autophagosome, and delivered to lysosomes for subsequent degradation. Autophagy is dependent on autophagy-related (ATG) proteins.<sup>1</sup> Autophagosome formation, elongation, and completion of enclosure require two ubiquitin-like conjugation systems: the first one generates the ATG5-ATG12 conjugate, which functions as a complex together with ATG16, and binds to the sequestering (pre-autophagosomal) phagophore. The second system conjugates an ATG8 homolog, LC3-I, with phosphatidylethanolamine to generate the lipidated LC3-II that associates with autophagosomes.<sup>2–4</sup> The conversion of LC3-I into LC3-II represents a hallmark of autophagic activity and is widely used for the detection of autophagosome formation. Another frequently used marker for monitoring autophagic activity is p62, a protein, which is specifically degraded through autophagy.<sup>5</sup>

The vital role of autophagy in cell growth, development, and homeostasis has long been appreciated. Recent data also indicate its involvement in the differentiation of hematopoietic cells. For instance, the importance of autophagy for efficient differentiation of leukocytes has been demonstrated with lymphocytes,<sup>6–8</sup> monocytes,<sup>9</sup> and dendritic cells,<sup>10</sup> as well as

reticulocytes.<sup>11,12</sup> Since granulopoiesis in the bone marrow is characterized by significant morphological changes and the acquisition of a range of effector functions, we hypothesized that autophagy might have a crucial role in the differentiation of neutrophils.

ATG5 is an essential protein for the elongation of pre-autophagosomal structures and subsequent autophagosome formation. Therefore, it represents a suitable genetic target for blocking autophagy. Using this strategy, we demonstrate here that neutrophil differentiation is controlled by autophagy, which in turn is negatively regulated by the p38 signaling pathway. Surprisingly, and in contrast to differentiation in other non-granulocytic hematopoietic lineages, autophagy was down-regulated during physiological neutrophil differentiation and its inappropriate induction delayed the differentiation process.

## Results

**Knocking out *Atg5* in the neutrophil lineage is associated with neutrophilia *in vivo*.** Because mice deficient for the gene encoding *Atg5* die within a few days after birth,<sup>13</sup> mice with a floxed *Atg5* allele were generated<sup>14</sup> to investigate the function of ATG5 *in vivo* in tissue-specific settings. We crossed mice bearing an *Atg5*<sup>flox</sup> allele, in which exon 3

<sup>1</sup>Institute of Pharmacology, University of Bern, Bern CH-3010, Switzerland and <sup>2</sup>Theodor Kocher Institute, University of Bern, Bern CH-3012, Switzerland

\*Corresponding author: HU Simon, Institute of Pharmacology, University of Bern, Friedbuehlstrasse 49, CH-3010 Bern, Switzerland. Tel: +41 31 632 3281; Fax: +41 31 632 4992; E-mail: hus@pki.unibe.ch

**Abbreviations:** ATG5, autophagy-related protein 5; *Atg5*Δ mouse, *Atg5*<sup>flox/flox</sup>-Lyz2Cre/Cre mouse; EdU, ethynyl deoxyuridine; Lyz2, lysozyme 2; 4-OHT, 4-hydroxytamoxifen; Hoxb8, homeobox b8; MMP, matrix metalloproteinase; mTORC, mammalian target of rapamycin complex; ROS, reactive oxygen species; SCF, stem cell factor; WT, wild type

Received 11.7.14; revised 04.9.14; accepted 09.9.14; Edited by G Kroemer; published online 17.10.14

of the *Atg5* gene is flanked by two *loxP* sequences (*Atg5<sup>fllox/fllox</sup>* mice)<sup>14</sup> with transgenic mice, expressing Cre recombinase under the control of the lysozyme 2 promoter, which is predominantly active in neutrophils, monocytes, and macrophages, but not in dendritic cells (*Lyz2<sup>Cre/Cre</sup>* mice).<sup>15</sup> Indeed, it has been earlier reported that macrophages of *Atg5<sup>fllox/fllox</sup>-Lyz2<sup>Cre/Cre</sup>* mice lack ATG5 expression and fail to kill intracellular pathogens.<sup>16</sup> In this study, we used *Atg5<sup>fllox/fllox</sup>-Lyz2<sup>Cre/Cre</sup>* mice to study the effects of *Atg5* deletion in the neutrophil lineage (designated *Atg5<sup>Δ</sup>* mice, henceforth). *Atg5<sup>fllox/fllox</sup>* and *Lyz2<sup>Cre/Cre</sup>* mice were used as controls throughout our experiments and are referred to as wild-type (WT) mice.

Mature bone marrow neutrophils of *Atg5<sup>Δ</sup>* mice displayed a complete *Atg5* knockout at the mRNA level, though in immature neutrophil populations small amounts of *Atg5* mRNA were detectable (Figure 1a). The latter might have been responsible for the traces of ATG5 protein barely detectable in mature bone marrow neutrophils (Figure 1b). The lack of ATG5 protein expression was at least partially specific for neutrophils, since neutrophil-depleted bone marrow cells clearly expressed ATG5 (Figure 1b). It should be noted, however, that a 70% reduction of ATG5 was also detectable in the neutrophil-depleted bone marrow fraction, most likely due to the presence of ATG5-deficient monocytes (mean 7.6%) and immature myelocytes (mean 4.7%), which demonstrated an incomplete reduction in ATG5 expression (Figure 1a). In addition, the neutrophil depletion was not complete in these experiments (10–12% remaining neutrophils).

Mature neutrophils from *Atg5<sup>Δ</sup>* mice exhibited reduced autophagic flux as assessed by p62 degradation (Figure 1b). Also, in contrast to WT neutrophils, mature neutrophils of *Atg5<sup>Δ</sup>* mice were unable to form autophagosomes, even when stimulated with rapamycin (Figure 1c). We conclude that mature neutrophils of *Atg5<sup>Δ</sup>* mice lack ATG5 and are autophagy deficient.

Autophagy-deficient, mature bone marrow neutrophils of *Atg5<sup>Δ</sup>* mice demonstrated a normal morphology and exhibited no difference in the release of granule proteins following *in vitro* activation as compared with neutrophils from WT mice (Supplementary Figure S1). In fact, we measured similar levels of cathepsin G (primary granules), lactoferrin (secondary granules), and MMP-9 (tertiary granules), suggesting that neutrophils of *Atg5<sup>Δ</sup>* mice contain the full spectrum of intact and fully matured granules after differentiation (Supplementary Figure S1).

We next measured neutrophil numbers and found elevated relative and absolute neutrophil numbers in the peripheral blood, lymph nodes, and spleen of *Atg5<sup>Δ</sup>* mice as compared with WT mice (Figure 2a, Supplementary Figure S2). In the bone marrow, relative, but not absolute neutrophil numbers were increased in association with the deficiency in neutrophil autophagy (Figure 2a, Supplementary Figure S2). It should be noted that monocyte/macrophage numbers did not significantly differ between *Atg5<sup>Δ</sup>* and WT mice (mean relative numbers of CD45<sup>+</sup>CD11b<sup>+</sup>CD115<sup>+</sup> cells: bone marrow, 8.11 versus 7.64%; blood, 3.43 versus 3.52%; spleen, 2.5 versus 2.1%; and lymph nodes, 0.65 versus 0.48%). We also did not observe significant differences in the numbers of B cells (mean

relative numbers of CD45<sup>+</sup>B220<sup>+</sup> cells: bone marrow, 25.9 versus 28.7%; blood, 48.2 versus 54.1%; spleen, 51.1 versus 50.7%; and lymph nodes, 44.1 versus 39.1%).

The differentiation of neutrophils is largely regulated by granulocyte colony-stimulating factor (G-CSF) and, to a lesser extent, by granulocyte/macrophage colony-stimulating factor (GM-CSF).<sup>17–19</sup> Therefore, we analyzed serum levels of G-CSF and GM-CSF; these, however, did not differ between *Atg5<sup>Δ</sup>* and WT mice (Supplementary Figure S3a). Increased neutrophil numbers of *Atg5<sup>Δ</sup>* mice were associated with significant splenomegaly and an increase in the ratio between spleen weight and total mouse weight (Supplementary Figure S3b). Histological analysis of the spleen revealed that, as in WT mice, neutrophils of *Atg5<sup>Δ</sup>* mice resided in the red pulp of the spleen, particularly in close proximity to the white pulp, in the area adjacent to the marginal zone (Supplementary Figure S3c).

Neutrophils of WT and *Atg5<sup>Δ</sup>* mice were equally recruited to the peritoneal cavity following intraperitoneal injection of IL-8, suggesting that an ATG5 deficiency does not result in a defect in migration in response to chemoattractants (Supplementary Figure S4a). We also performed *in vitro* experiments to test whether ATG5-deficient neutrophils exhibit any functional defects. Analyzing the stimulated production of reactive oxygen species (ROS) by mature bone marrow neutrophils, as well as their capacity to phagocytose and to kill bacteria revealed no differences between *Atg5<sup>Δ</sup>* and WT mice (Supplementary Figure S4b–d), suggesting that ATG5 or autophagy in these cells is not required for their effector functions within the innate immune system.

### Knocking out *Atg5* in the neutrophil lineage is associated with increased and more rapid neutrophil production *in vivo*.

We evaluated the proliferative status of neutrophil precursors in the bone marrow, using the Ki-67 marker, which is expressed in actively proliferating cells, but absent in resting cells (G<sub>0</sub>).<sup>20</sup> At the early promyelocytic/myelocytic stages of neutrophil differentiation, it is known that cells rapidly proliferate, thus forming a pool of immature neutrophil precursors. The proliferation ceases as these cells mature into metamyelocytes, band cells, and segmented neutrophils.<sup>21,22</sup> The mitotic pool of immature neutrophil precursors in the bone marrow of *Atg5<sup>Δ</sup>* mice exhibited a significantly higher proliferation rate when compared with WT mice, whereas the proliferation rate of mature neutrophils was, as expected, comparably low in all genotypes (Figure 2b). *Atg5* mRNA expression in these immature neutrophil populations was reduced by 75.3 ± 18.9% compared with WT mice (Figure 1a). These data indicate that ATG5 limits proliferation of immature neutrophils under *in vivo* conditions.

To assess the kinetics of differentiation of neutrophil precursors *in vivo*, we examined the blood of WT and *Atg5<sup>Δ</sup>* mice after a pulse of ethynyl deoxyuridine (EdU), a nucleotide analog of thymidine that incorporates into the DNA of dividing cells.<sup>23</sup> EdU incorporation into the proliferating neutrophil precursors in the bone marrow allowed us to chase EdU<sup>+</sup> neutrophils reaching the blood stream after maturation. The egress of EdU<sup>+</sup> neutrophils of *Atg5<sup>Δ</sup>* mice from the bone marrow into the blood stream started already after 48 h and

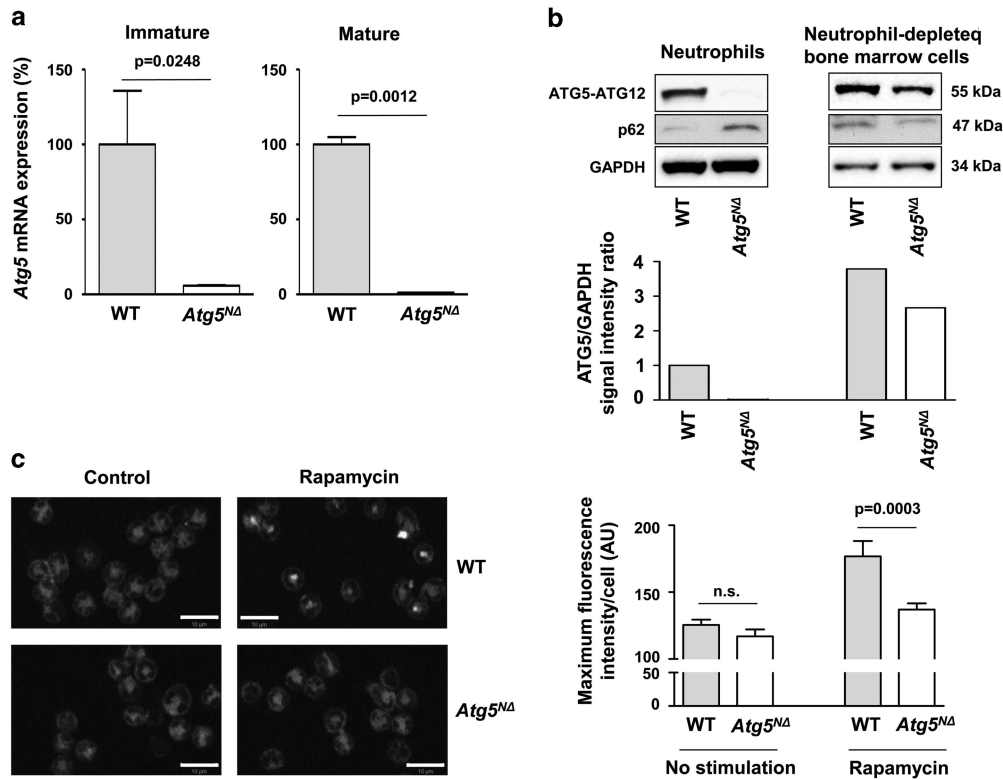


**Figure 1** Lack of *Atg5* mRNA and ATG5 protein expression as well as a functional defect in autophagy in neutrophils of *Atg5<sup>NΔ</sup>* mice. (a) Quantitative real-time PCR. Freshly purified immature and mature bone marrow-derived neutrophil samples from WT and *Atg5<sup>NΔ</sup>* mice were analyzed for *Atg5* expression. S18 was used as a reference gene to normalize the expression of *Atg5*. Values are means  $\pm$  S.E.M. of two independent experiments. (b) Immunoblotting. Freshly purified mature bone marrow-derived neutrophils of WT and *Atg5<sup>NΔ</sup>* mice were analyzed for ATG5 protein expression. The neutrophil-depleted bone marrow samples were lysed and immunoblotted next to the neutrophil lysates to demonstrate the cell specificity of the ATG5 knockout. If present, ATG5 protein is seen as a conjugate with ATG12. The accumulation of p62 confirms the attenuated autophagic activity in ATG5-deficient neutrophils. The results are representative of three independent experiments. The quantification of the ATG5 signal was performed using the Odyssey Fc Imaging System (LI-COR Biosciences GmbH, Bad Homburg, Germany) and the image Studio software. (c) Confocal microscopy. Freshly purified mature bone marrow-derived neutrophils of WT and *Atg5<sup>NΔ</sup>* mice were cultured in the presence and absence of rapamycin for 1 h and stained with AUTodot autophagy visualization dye. The dye is specific for autophagic vacuoles that can be detected in rapamycin-treated WT neutrophils as bright white dots. In contrast, rapamycin had no detectable effect on neutrophils derived from *Atg5<sup>NΔ</sup>* mice. Bars, 10  $\mu$ m. (Right) Statistical analysis of three independent confocal microscopy experiments. Values are means  $\pm$  S.E.M.

reached its peak at 72 h following the pulse (Figure 2c). In contrast, in WT mice, the maximum output of EdU<sup>+</sup> neutrophils was detected after 96 h (Figure 2c). The observed earlier output of EdU<sup>+</sup> neutrophils in *Atg5<sup>NΔ</sup>* mice suggests an increased proliferation of the mitotic pool and an accelerated maturation of the post-mitotic pool of ATG5-deficient neutrophils as compared with normal neutrophils.

Autophagy is tightly linked to the survival of cells and their susceptibility to undergoing cell death. The kinetics of *in vitro* cell death, however, did not differ between ATG5-deficient and WT mature blood or bone marrow neutrophils (Supplementary Figure S5a and b). Both ATG5-deficient and WT mature bone marrow neutrophils could be protected from cell death by the addition of the broad spectrum caspase inhibitor Q-VD-OPh, indicating that apoptosis was the predominant form of cell death regardless of ATG5 expression levels (Supplementary Figure S5b). Taken together, our findings indicate that the lack of ATG5 in the neutrophil lineage results in a neutrophilia that is the consequence of both increased and accelerated, but cytokine-independent, neutrophil production, rather than being due to a reduced cell death.

**ATG5 regulates neutrophil differentiation *in vitro*.** To investigate whether the accelerated neutrophil production observed in *Atg5<sup>NΔ</sup>* mice is direct, and if so, its underlying mechanism, we performed *in vitro* studies. To this end, we employed stem cell factor (SCF)-dependent conditional Hoxb8 neutrophils (Hoxb8 neutrophils, henceforth), which represent 4-hydroxytamoxifen (4-OHT)-regulated mouse neutrophil progenitors that undergo normal neutrophil differentiation upon *Hoxb8* inactivation (Supplementary Figure S6a).<sup>24,25</sup> During the differentiation process, the cells upregulate expression of neutrophil cell surface markers, such as Gr-1 and CD11b, and concurrently downregulate the SCF receptor (c-KIT, CD117) (Supplementary Figure S6b). Gelatinase B/matrix metalloproteinase 9 (MMP-9) is an enzyme present in tertiary neutrophil granules, which are identified by their late appearance in myeloid differentiation.<sup>26</sup> As Hoxb8 neutrophil precursors mature, the expression of MMP-9 is gradually upregulated and no difference in MMP-9 expression levels was detectable as compared with primary mature bone marrow neutrophils after reaching full maturation (Supplementary Figure S6c). Hoxb8 neutrophils were

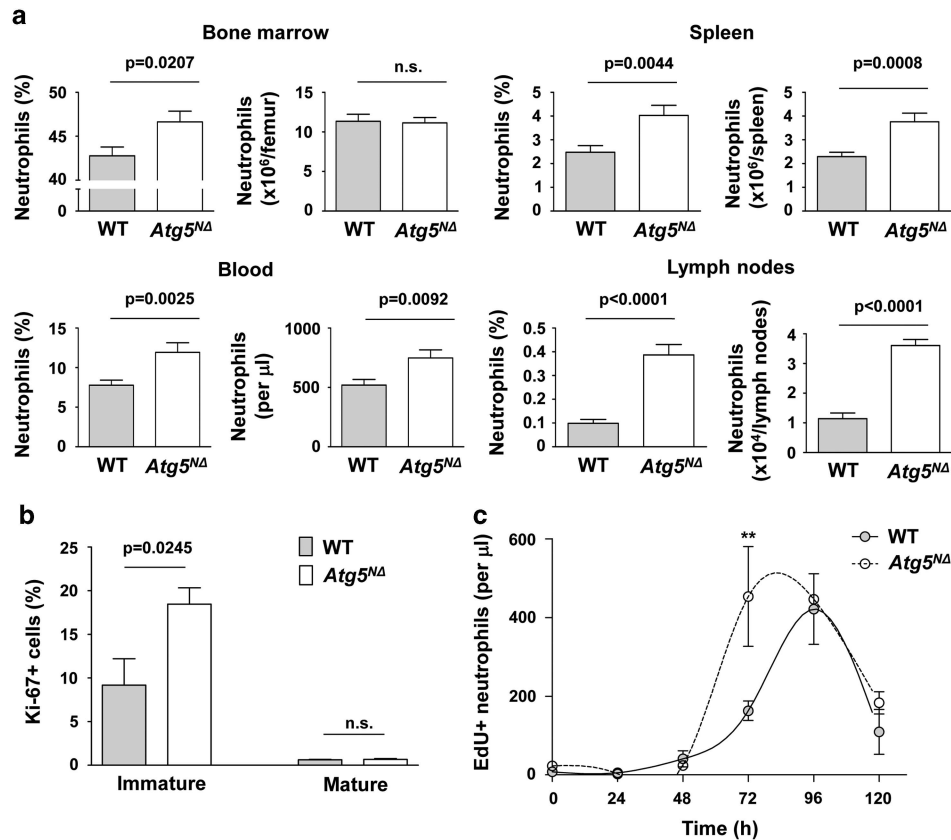


**Figure 2** Increased proliferation and granulopoiesis of neutrophil precursors in the bone marrow of *Atg5<sup>NA</sup>* mice. (a) Flow cytometry. Relative and absolute neutrophil numbers in bone marrow, peripheral blood, spleen, as well as brachial and axillary lymph nodes of WT and *Atg5<sup>NA</sup>* mice. Values are means  $\pm$  S.E.M. ( $n=10-15$ ). The gating strategy and representative examples of the measurements are shown in Supplementary Figure S2. (b) Flow cytometry. The proliferative status of immature neutrophil precursors in the bone marrow of WT and *Atg5<sup>NA</sup>* mice was assessed with Ki-67 expression measurements. Values are means  $\pm$  S.E.M. ( $n=3$ ). The precursors were defined as CD11b<sup>+</sup>Ly6G<sup>-</sup>CD115<sup>+</sup>SSC<sup>high</sup> and mature neutrophils as the CD11b<sup>+</sup>Ly6G<sup>+</sup> cell population (see Supplementary Figure S2a and b). (c) Flow cytometry. Absolute numbers of EdU<sup>+</sup> neutrophils in the blood of WT and *Atg5<sup>NA</sup>* mice were measured at indicated time points after EdU injection. Values are means  $\pm$  S.E.M. ( $n=3-6$ ). \*\* $P < 0.01$

also functionally competent and performed basic neutrophil effector functions, such as phagocytosis and ROS production, with no detectable difference as compared with primary mature bone marrow neutrophils (Supplementary Figure S6d), confirming previously published work.<sup>24,25</sup>

We transduced Hoxb8 neutrophils with a lentiviral vector expressing Tet-regulated shRNA for the knockdown of *Atg5* mRNA transcripts. In this inducible system, the shRNA *Atg5* production was regulated by the presence or absence of doxycycline. Upon a 24-h doxycycline treatment, we observed an approximately 40% downregulation of *Atg5* mRNA (Figure 3a). Moreover, ATG5 protein expression was reduced; similarly, autophagic activity decreased as reflected by reduced LC3-II and increased p62 levels, respectively (Figure 3b). The shRNA *Atg5* Hoxb8 neutrophils were always compared with control Hoxb8 neutrophils, which had been transduced with a control shRNA vector. The control and *Atg5*-downregulated neutrophil progenitors were at the same stage of differentiation when kept in 4-OHT-containing culture medium, having the morphological and biomolecular characteristics of promyelocytes (Supplementary Figure S7a and b). After downregulating the expression of *Atg5* (0.1  $\mu$ g/ml doxycycline for 24 h), the differentiation process was initiated by removing 4-OHT. Immature Hoxb8 neutrophils with reduced ATG5 expression

demonstrated an accelerated differentiation process as assessed by morphology (Figure 3c), as well as Gr-1 (Figure 3d) and MMP-9 expression (Figure 3e).

Next, using lentiviral transduction, we generated *Atg5*-overexpressing Hoxb8 neutrophils that were compared with Hoxb8 neutrophils transduced with a control empty vector (Figures 4a and b). Again, when kept in 4-OHT-containing culture medium, both neutrophil lines were at the same, promyelocytic stage of differentiation (Supplementary Figure S7c and d). The ATG5-overexpressing immature neutrophils exhibited increased autophagic activity compared with control Hoxb8 precursors, as was evident from increased LC3-II and reduced p62 levels, respectively (Figure 4b). After the initiation of the differentiation process, immature Hoxb8 neutrophils with increased ATG5 expression demonstrated a delayed differentiation process as assessed by morphology (Figure 4c), as well as Gr-1 (Figure 4d) and MMP-9 expression (Figure 4e). Taken together, these data suggest that ATG5, in modulating autophagy, impacts neutrophil differentiation in a cell autonomous manner.

**Neutrophil differentiation is regulated by autophagy.** The observation that ATG5 levels influence the process of neutrophil differentiation suggested that autophagy



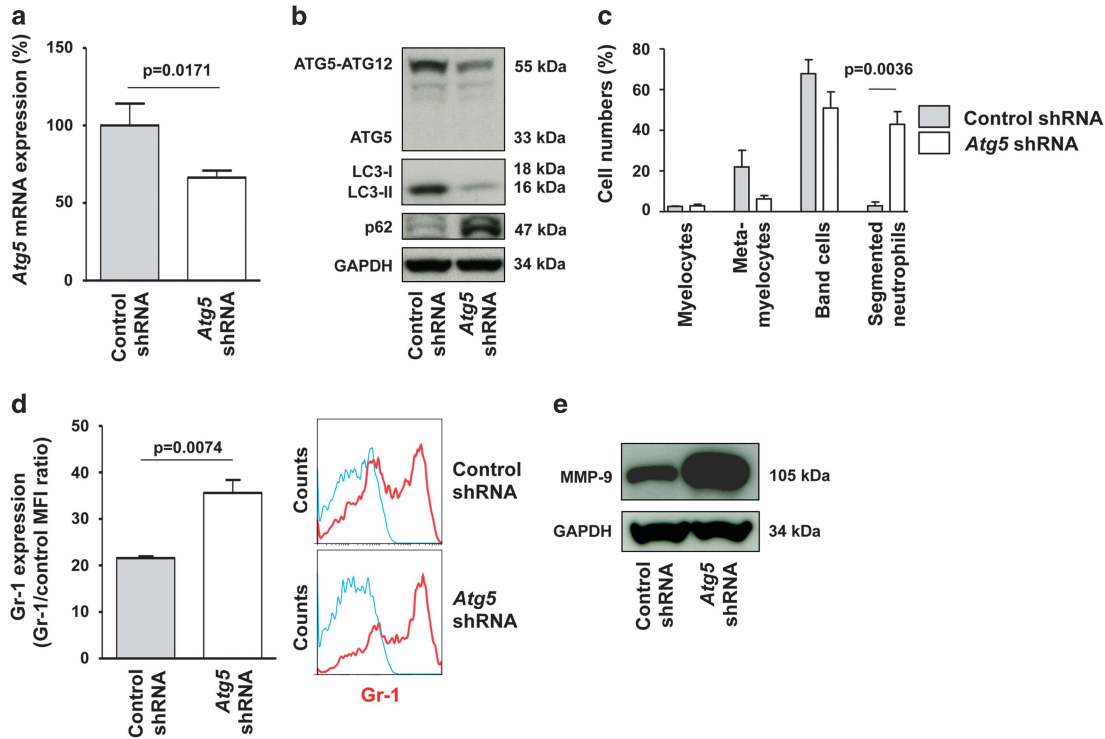


**Figure 3** Downregulation of ATG5 expression in immature neutrophil precursors results in accelerated differentiation. (a) Quantitative real-time PCR. Undifferentiated Hoxb8 neutrophils were transduced with virus encoding control or *Atg5*-specific shRNA, and subsequently analyzed. S18 was used as a reference gene to normalize the expression of *Atg5*. Values are means  $\pm$  S.E.M. of three independent experiments. (b) Immunoblotting. ATG5 expression is decreased in *Atg5* shRNA-treated undifferentiated Hoxb8 neutrophils. Monomeric ATG5 was not detectable in these cells. The reduced presence of the ATG5-ATG12 conjugate was correlated with reduced LC3-II and higher p62 levels, indicating attenuated autophagic activity in these cells. Results are representative of three independent experiments. (c) Light microscopy. Undifferentiated Hoxb8 neutrophils were treated with control or *Atg5* shRNA and then allowed to differentiate for 4 days. Cytospins were stained with the Hematoxylin and Eosin (H&E) and quantified. Based on cell size and nuclear morphology, cells were categorized as myelocytes, metamyelocytes, band cells, or segmented neutrophils. Values are means  $\pm$  S.E.M. of three independent experiments. (d) Flow cytometry. Undifferentiated Hoxb8 neutrophils were treated with control and *Atg5* shRNA, allowed to differentiate for 3 days, and Gr-1 surface expression analyzed. Values are means  $\pm$  S.E.M. of four independent experiments. (Right) Representative original flow cytometric data are shown. Red, Gr-1 expression. Blue, isotype-specific control antibody staining. (e) Immunoblotting. Undifferentiated Hoxb8 neutrophils were treated with control and *Atg5* shRNA, allowed to differentiate for 4 days, and MMP-9 expression analyzed. Results are representative of three independent experiments. See Supplementary Figure S6 for the characterization of the Hoxb8 neutrophil differentiation system

participates in the regulation of this process. To address this question, we analyzed Hoxb8 neutrophils during the differentiation process from promyelocytes to mature neutrophils. As assessed with LC3 and p62 immunoblotting, we found an increased autophagic activity in promyelocytes and myelocytes compared with later stages of neutrophil differentiation (Figure 5a). In fact, autophagy appeared to decline at day 3 after the initiation of the differentiation process (Figure 5a). By this time point, cells had largely matured into metamyelocytes and band cells (Supplementary Figure S6a). The lowest levels of autophagy were observed at day 5 (Figure 5a), a time point by which all cells had undergone terminal differentiation (Supplementary Figure S6a). These data support our observation that a reduction in ATG5 expression (and, thereby, a reduction in autophagy) promotes the differentiation process of neutrophils (Figure 3). The physiological process of autophagy during neutrophil differentiation, however, does not appear to be regulated by modulating ATG5 expression levels (Figure 5a). Similarly, the expression of Beclin 1 (ATG6) did not change significantly during neutrophil differentiation (Figure 5a).

Therefore, we searched for other candidates that might be regulating the process of autophagy during the differentiation of neutrophils. Mammalian target of rapamycin complex 1 (mTORC1) is known to be a key regulator of autophagy. mTORC1 activity inhibits autophagy and is regulated by availability of nutrients and growth factors and by other upstream signaling pathways.<sup>27,28</sup> We analyzed the activation level of mTORC1 by monitoring phosphorylation of p70S6 kinase (p70S6K), a well-characterized mTORC1 target that regulates protein synthesis by phosphorylating the S6 ribosomal protein.<sup>29,30</sup> In correlation with the observed decrease in autophagic activity during neutrophil differentiation, the levels of phosphorylated p70S6K increased as neutrophils matured (Figure 5a, lower panel).

To demonstrate functionally the importance of mTORC1 for regulation of autophagy and neutrophil differentiation, rapamycin was used to directly inhibit mTORC1. Indeed, rapamycin blocked mTORC1 and, as expected, induced autophagy (Figure 5b). As observed with ectopically ATG5-induced autophagy, rapamycin-induced autophagy also drastically blocked neutrophil differentiation as assessed by flow cytometric surface Gr-1 expression (Figure 5c). Similarly,

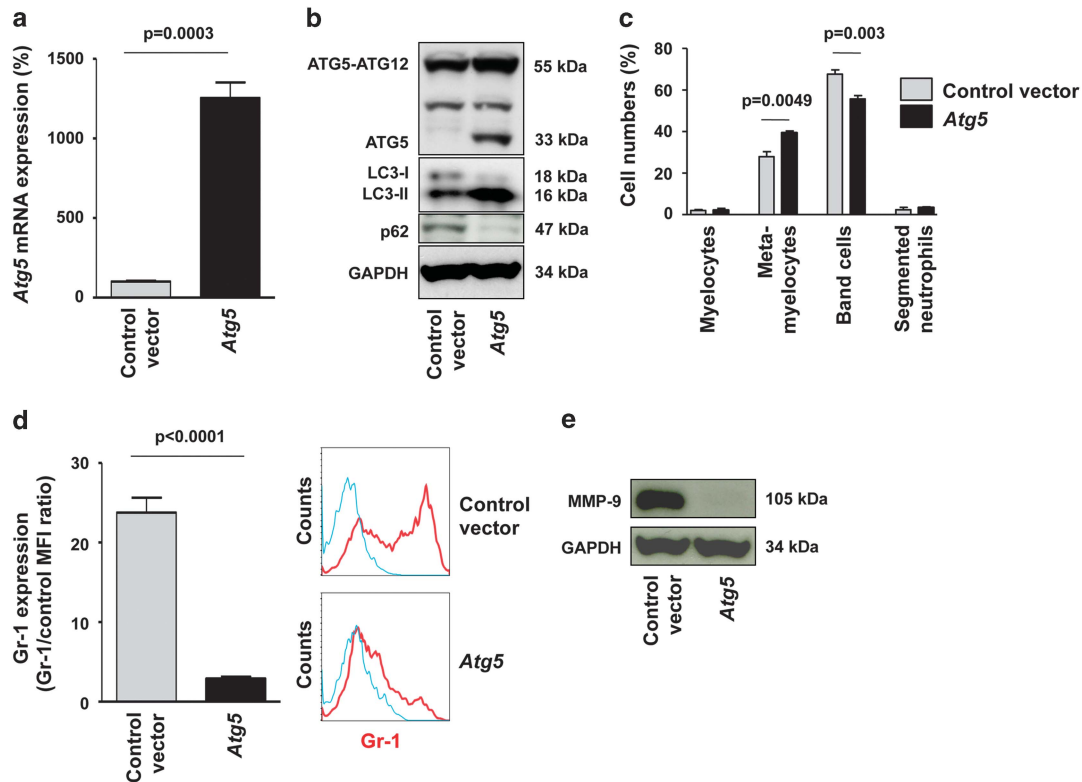


**Figure 4** Ectopic *Atg5* expression in immature neutrophil precursors results in delayed differentiation. (a) Quantitative real-time PCR. Undifferentiated Hoxb8 neutrophils were subjected to lentiviral transduction with control vector or *Atg5* gene construct, and subsequently analyzed. *S18* was used as a reference gene to normalize the expression of *Atg5*. Values are means  $\pm$  S.E.M. of three independent experiments. (b) Immunoblotting. *Atg5* gene transfer results in strong expression of the 33-kDa ATG5 monomer and slightly increased expression of ATG5 within the conjugate with ATG12. Ectopic ATG5 expression was associated with higher LC3-II and reduced p62 levels, suggesting increased autophagic flux in these cells. Results are representative of three independent experiments. (c) Light microscopy. Undifferentiated Hoxb8 neutrophils were subjected to lentiviral control vector and *Atg5* gene transfer and then allowed to differentiate for 4 days. Cytospins were stained with the Hemacolor Set and quantified. Based on cell size and nuclear morphology, cells were categorized as myelocytes, metamyelocytes, band cells, or segmented neutrophils. Values are means  $\pm$  S.E.M. of three independent experiments. (d) Flow cytometry. Undifferentiated Hoxb8 neutrophils were subjected to lentiviral control vector and *Atg5* gene transfer, allowed to differentiate for 3 days, and the Gr-1 expression analyzed. Values are means  $\pm$  S.E.M. of four independent experiments. (Right) Representative original flow cytometric data are shown. Red, Gr-1 expression. Blue, isotype-matching control antibody. (e) Immunoblotting. Undifferentiated Hoxb8 neutrophils were subjected to lentiviral control vector and *Atg5* gene transfer, allowed to differentiate for 4 days, and MMP-9 expression analyzed. Results are representative of three independent experiments. See Supplementary Figure S6 for the characterization of the Hoxb8 neutrophil differentiation system

trifluoperazine and carbamazepine, two other known autophagy-inducing drugs,<sup>31–33</sup> also inhibited the differentiation of neutrophils (Supplementary Figure S8). In summary, autophagy appears to have a counter-regulatory role in the process of neutrophil differentiation.

**Autophagy and neutrophil differentiation underlie a reciprocal regulation by p38.** To determine the upstream signals responsible for an autophagic regulation of differentiation for neutrophil precursors, we studied several pathways converging at mTORC1. Class I phosphatidylinositol 3-kinases (PI3K-I) activate phosphoinositide dependent protein kinase-1 (PDK1) in the PI3K-I/PDK1/protein kinase B (AKT) signaling pathway, which is known to suppress autophagy by activating mTORC1.<sup>34,35</sup> However, we obtained no evidence for the activation of this pathway during differentiation of Hoxb8 neutrophils (Supplementary Figure S9a) and pharmacological inhibition of PI3K-I or AKT kinase had no effect on the generation of mature neutrophils as assessed by flow-cytometric surface Gr-1 expression (Supplementary Figure S9b).

On the other hand, mTORC1 can also be activated by the p38 MAPK cascade through inhibition of tuberlin (TSC2), a critical negative regulator of mTORC1.<sup>36</sup> Indeed, the phosphorylation of p38 increased during differentiation of Hoxb8 neutrophils and was the highest in band cells and fully mature neutrophils (Figure 6a). Pharmacological inhibition of the p38 pathway with the specific p38 inhibitor PD169316 induced autophagy (Figure 6b) and drastically inhibited neutrophil differentiation as assessed by flow-cytometric surface Gr-1 expression (Figure 6c). Inhibiting the p38 pathway also caused the inhibition of p70S6K phosphorylation (Figure 6d), thus verifying mTORC1 as the molecular link between activated p38 and autophagy inhibition. In contrast to p38, ERK1/2 phosphorylation was reduced at later differentiation stages of Hoxb8 neutrophils (Figure 6a) and blocking the ERK1/2 signaling pathway with the ERK pathway inhibitor SD98059 had no effect on neutrophil differentiation (Figure 6c). In summary, these results demonstrate that neutrophil differentiation and autophagy are reciprocally regulated by the p38-mTORC1 pathway, whereas the PI3K and ERK signaling pathways do not seem to have a role.

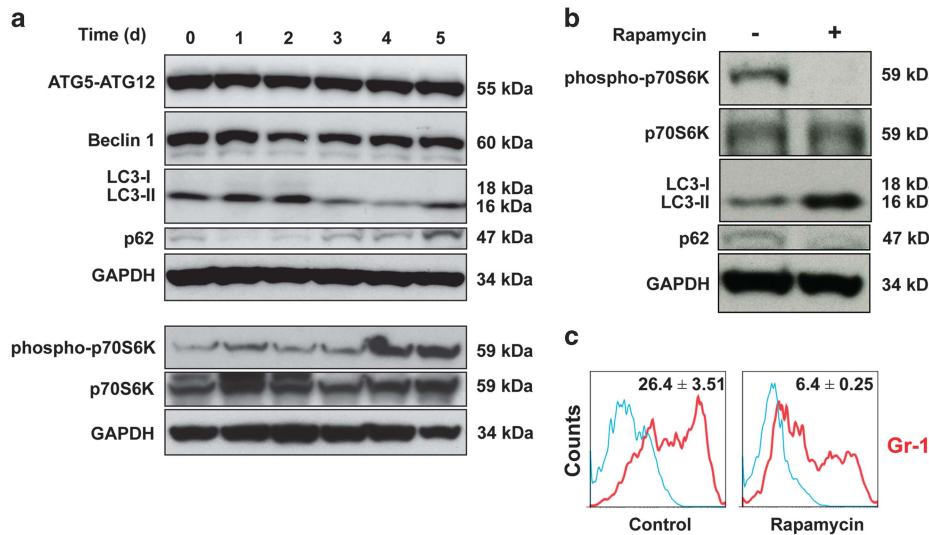


**Figure 5** Autophagic activity declines during neutrophil differentiation and pharmacological induction of autophagy delays the process of neutrophil differentiation. (a) Immunoblotting. Hoxb8 neutrophil progenitors were allowed to differentiate and analyzed at the indicated times (see Supplementary Figure S6 for the characterization of the Hoxb8 neutrophil differentiation system). The autophagic activity appeared to decline at later time points as indicated by reduced LC3-II and higher p62 levels. ATG5 and Beclin 1 expression did not change during the process of neutrophil differentiation. However, phosphorylation (Thr389) of p70S6K increased, suggesting increased mTORC1 activity. Results are representative of four independent experiments. (b) Immunoblotting. Hoxb8 neutrophil progenitors were allowed to differentiate in the presence and absence of 100 nM rapamycin and analyzed 3 days after initiation of the differentiation process. Rapamycin treatment resulted in higher LC3-II and reduced p62 levels, suggesting induction of autophagy. The results are representative of two independent experiments. (c) Flow cytometry. Hoxb8 neutrophil progenitors were allowed to differentiate in the presence and absence of 100 nM rapamycin and analyzed 3 days after initiation of the differentiation process. Rapamycin treatment resulted in lower Gr-1 surface expression, suggesting a delayed differentiation process as a consequence of autophagy induction. Representative original flow cytometric data are shown. Red, Gr-1 expression. Blue, isotype-matching control antibody. The indicated values are mean Gr-1/control MFI ratios  $\pm$  S.E.M. of four independent experiments

## Discussion

Although autophagy has been implicated in innate and adaptive immune responses,<sup>37</sup> its role in neutrophil biology has not been investigated previously. In this study, we report that ATG5-deficient neutrophils exhibit normal effector functions (ROS production, phagocytosis, granule protein release, and bacterial killing), at least under *in vitro* conditions. On the other hand, we demonstrate that autophagy contributes to the regulation of neutrophil numbers by modulating their production in the bone marrow. However, ATG5-deficient neutrophils do not display any differences in their survival and rates of spontaneous apoptosis. Delayed apoptosis in the presence of survival cytokines was also not dependent on the presence of ATG5. These data suggest that autophagy can modulate neutrophil numbers solely at the level of production, but not by regulating the apoptosis of mature neutrophils.

Using genetic and pharmacological, as well as combined *in vivo* and *in vitro* approaches, we show that autophagy limits and delays neutrophil differentiation, a finding that was largely unexpected, since previously published work consistently suggested an essential role for autophagy in the process of differentiation of multiple hematopoietic and non-hematopoietic cells. For instance, autophagy has been demonstrated to be required for organelle clearance during the differentiation of reticulocytes.<sup>12,38</sup> Similarly, B-cell differentiation was blocked at the pro-B cell stage in bone marrow in the absence of ATG5.<sup>8</sup> ATG5-deficient B cells were also unable to differentiate to plasma cells.<sup>39</sup> Furthermore, autophagy is required during monocyte differentiation and acquisition of macrophage effector functions<sup>9,40</sup> as well as for

megakaryocyte differentiation.<sup>41</sup> Autophagy has also been shown to maintain hematopoietic stem cells.<sup>42–44</sup> In addition, a requirement for autophagy in differentiation has been reported in non-hematopoietic cells, such as adipocytes<sup>45–47</sup> and osteoblasts.<sup>48</sup>

Differentiation is associated with rapid cellular changes. Our findings provoke the question: Why is such a cellular remodeling process not required during neutrophil differentiation as is obviously the case in other cell lineages? The major changes that appear during neutrophil differentiation are cytoplasmic granule formation and changes in nuclear morphology. We found no evidence that ATG5-deficient mature neutrophils obtained from *Atg5<sup>Δ</sup>* mice were different from mature neutrophils of WT mice in terms of granule composition or nuclear morphology. It is possible that the numbers of mitochondria are increased as a consequence of the absence of ATG5, but, even if this were to be the case, it did not affect neutrophil morphology or function. Perhaps, due to the relatively short life span of mature neutrophils, the removal of mitochondria is less crucial than with reticulocytes.<sup>11,12</sup> The short life span may also explain why mature neutrophils, as post-mitotic cells, apparently do not require active autophagy for cellular homeostasis as is, for example, the case in neurons.<sup>14,49</sup>

Interestingly, it has been shown that the induction of autophagy is required for the differentiation of acute myeloid leukemia (AML) cells.<sup>50,51</sup> The accelerated differentiation might be explained, at least partially, by the autophagic degradation of the driving oncoprotein.<sup>52</sup> The question arises, whether the induction of differentiation by autophagy regulators is differently regulated in AML cells than in healthy

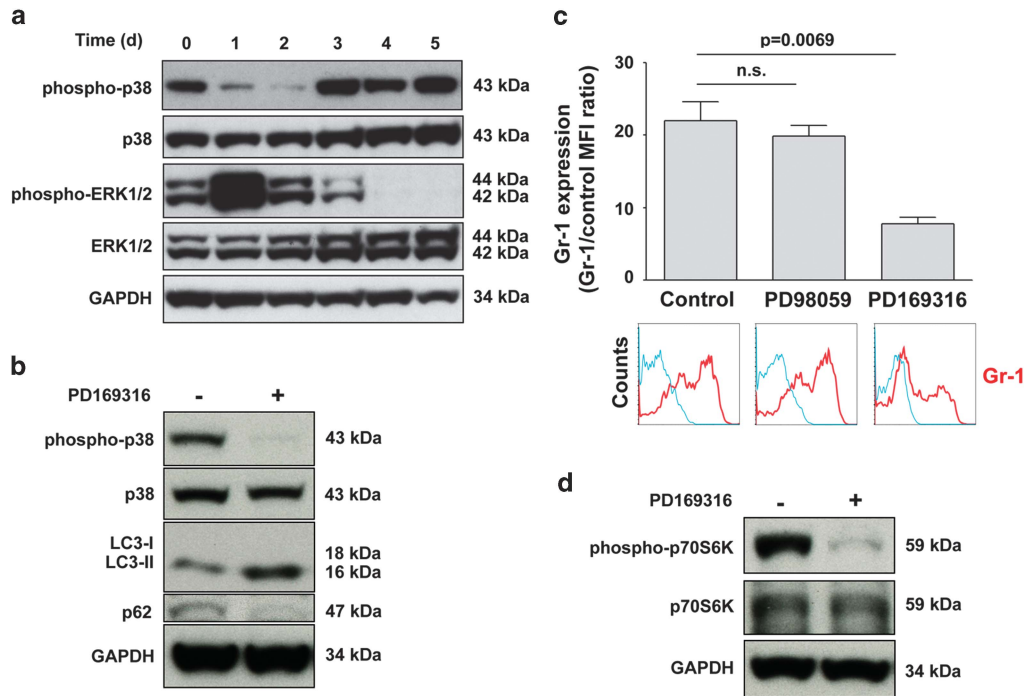


**Figure 6** Activity of p38 increases during neutrophil differentiation and its pharmacological inhibition induces autophagy and reduces the process of neutrophil differentiation. (a) Immunoblotting. Hoxb8 neutrophil progenitors were allowed to differentiate and analyzed at the indicated times (see Supplementary Figure S6 for the characterization of the Hoxb8 neutrophil differentiation system). Phosphorylation (Thr180/Tyr182) of p38 increased, suggesting increased p38 activity. On the other hand, ERK1/2 was completely dephosphorylated (Thr202/Thr204) during terminal differentiation. Results are representative of four independent experiments. We obtained no evidence for a role for the PI3K pathway in neutrophil differentiation (see Supplementary Figure S9). (b) Immunoblotting. Hoxb8 neutrophil progenitors were allowed to differentiate in the presence and absence of 1  $\mu$ M PD169316 (inhibitor of p38), and analyzed 3 days after initiation of the differentiation process. PD169316 treatment resulted in higher LC3-II and lower p62 levels, indicating induction of autophagy. The results are representative of two independent experiments. (c) Flow cytometry. Hoxb8 neutrophil progenitors were allowed to differentiate in the presence and absence of 1  $\mu$ M PD169316 (inhibitor of p38) or 1  $\mu$ M PD98059 (inhibitor of ERK1/2), and analyzed 3 days after initiation of the differentiation process. PD169316 treatment resulted in lower Gr-1 surface expression, suggesting a delayed differentiation process as a consequence of autophagy induction. In contrast, pharmacological inactivation of ERK1/2 had no effect in this system. Values are means  $\pm$  S.E.M. of four independent experiments. Representative original flow cytometric data are shown below. Red, Gr-1 expression. Blue, isotype-matching control antibody. (d) Immunoblotting. Hoxb8 neutrophil progenitors were allowed to differentiate in the presence and absence of 1  $\mu$ M PD169316 (inhibitor of p38), and analyzed 3 days after initiation of the differentiation process. PD169316 treatment resulted in decreased phosphorylation (Thr389) of p70S6K, suggesting diminished mTORC1 activity. Results are representative of two independent experiments

immature neutrophils, a possibility which, if true, could open up new avenues for treatment of AML. However, it has also been reported that inhibition of autophagy by chloroquine enhanced AML cell differentiation,<sup>53</sup> pointing to the possibility that AML cell and neutrophil differentiation are not really differently regulated, since in both cases differentiation seems to be promoted by a reduction in autophagy.

Although the data obtained in *Atg5<sup>MΔ</sup>* mice clearly indicate that autophagy is not required for the later differentiation processes of neutrophils, our Hoxb8 neutrophil system allowed us to follow in detail the levels of autophagy associated with neutrophil differentiation, at least from the promyelocytic stage onwards until terminal differentiation. The highest autophagic activity was observed during early granulopoiesis, at the promyelocytic and myelocytic stages of differentiation. At the transition from myelocytes to metamyelocytes and in mature neutrophils, autophagy appeared to decline. Interestingly, these changes in autophagic activity were associated with increased p38 and decreased ERK1/2 phosphorylation levels. Using a pharmacological approach, we demonstrated that autophagy in neutrophils, and reciprocally in consequence, differentiation, are regulated by the p38–mTORC1 axis. Our data for the importance of p38

in the regulation of neutrophil differentiation are in agreement with previously published work demonstrating that the phosphatase Wip1 blocks the differentiation process of neutrophils through the inhibition of the p38 MAPK-STAT1 pathway.<sup>54</sup> In addition, neutropenia has been recognized as an important adverse event of rapamycin therapy,<sup>55</sup> pointing to the possibility that mTOR-regulated autophagy in neutrophil precursors is responsible for this phenomenon.

The proliferation of immature neutrophils at the promyelocytic/myelocytic stages inversely correlated with levels of autophagy under *in vivo* conditions. Previously published work reported that the deletion of *Atg7* in the hematopoietic system results in a severe myeloproliferation,<sup>43</sup> a finding that supports the assumption that autophagy negatively regulates the proliferation of myeloid precursor cells. Moreover, similar observations have been made in melanoma cells,<sup>56</sup> as well as in lung and breast cancer cells.<sup>57,58</sup> Furthermore, autophagy and p38 have been demonstrated to have an important role in mediating senescence.<sup>59,60</sup> Similarly, ATG7, another protein essential for autophagosome formation, has been shown to be essential for cell-cycle arrest.<sup>61</sup> The molecular mechanisms whereby autophagy mediates anti-proliferative effects remain unclear. However, modulation of key autophagic components



such as ULK3, ATG5, or ATG7 has been shown to control senescence, possibly through feedback control of the PI3K-AKT-mTOR pathway.<sup>62</sup> On the other hand, more direct effects of autophagy on the regulation of mitosis by degradation of active RHOA<sup>63</sup> or ATG5–survivin interactions in the nucleus<sup>64</sup> may also have a role. Moreover, both ATG5<sup>65</sup> and ATG7<sup>61</sup> have been shown to increase p53 expression and/or function that could also have a role in the initiation of senescence.

Taken together, our findings indicate that autophagy negatively impacts on neutrophil differentiation. Interestingly, our work may explain why p73 knockout mice suffer from a general neutrophilic inflammation,<sup>66</sup> since these mice exhibit strongly reduced ATG5 levels in multiple cell lineages.<sup>67</sup> Reduced ATG5 levels in immature neutrophils clearly stimulate neutrophil production as demonstrated in this work. We further show that autophagy is regulated, at least partially, by the p38–mTORC1 signaling pathway. Autophagy-deficient neutrophils exhibit normal morphology and no evidence for a defect in granule protein release or a deregulation in apoptosis. Further work is required to rule out the possibility that autophagy-deficient neutrophils exhibit other functional abnormalities. Moreover, the potential for modulating autophagy in immature neutrophils with drugs should be explored as an option for normalizing neutrophil numbers under pathological conditions.

## Materials and Methods

**Antibodies.** The antibodies used for immunoblotting were polyclonal rabbit anti-ATG5 (1 : 500; Novus Biologicals, LuBioScience GmbH, Lucerne, Switzerland), polyclonal rabbit anti-p62 (1 : 4000; Novus Biologicals), monoclonal mouse anti-LC3 (1 : 500; Nanotools, Teningen, Germany), monoclonal mouse anti-Beclin 1 (1 : 1000; Abgent, LuBioScience GmbH), polyclonal rabbit anti-MMP-9 (1 : 1000; Abcam, Cambridge, UK), and monoclonal mouse anti-GAPDH (1 : 5000; Millipore, Bedford, MA, USA). From Cell Signaling Technology (Danvers, MA, USA), we obtained the following antibodies for immunoblotting: monoclonal rabbit anti-phospho-p70S6K (1 : 500), monoclonal rabbit anti-p70S6K (1 : 500), polyclonal rabbit anti-phospho-p38 (1 : 1000), polyclonal rabbit anti-p38 (1 : 1000), monoclonal rabbit anti-phospho-ERK1/2 (1 : 1000), monoclonal rabbit anti-ERK1/2 (1 : 1000), polyclonal rabbit anti-phospho-PDK1 (1 : 1000), polyclonal rabbit anti-PDK1 (1 : 1000), polyclonal rabbit anti-phospho-Akt (1 : 1000), and polyclonal rabbit anti-Akt (1 : 1000). Horseradish peroxidase (HRP)-conjugated goat anti-mouse and HRP-conjugated donkey anti-rabbit antibodies were from GE Healthcare (Little Chalfont, UK). The antibodies against cell surface markers used for flow cytometry and cell sorting were all rat anti-mouse antibodies directed against CD45, Ly6G, CD11b, CD115, Gr-1, and c-KIT (all from Biolegend, Lucerna-Chem AG, Lucerne, Switzerland). The rat IgG2b,  $\kappa$  isotype control was from Biolegend (Lucerna-Chem AG). The polyclonal rabbit anti-Ki-67 for intracellular staining was from Abgent (LuBioScience GmbH) and the rabbit IgG isotype control was from Novus Biologicals. PerCP-conjugated goat-anti-rabbit antibody was from Santa Cruz Biotechnology (Santa Cruz, Labforce AG, Nunningen, Switzerland).

**Reagents.** RPMI-1640/GlutaMAX medium and penicillin/streptomycin were from Invitrogen (LuBioScience GmbH). All media were supplemented with 10% fetal calf serum (FCS) (GE Healthcare). Q-VD-OPh was from SM Biochemicals (Anaheim, CA, USA).  $\beta$ -Mercaptoethanol, 4-OHT, hexadimethrine bromide (polybrene) and puromycin were from Sigma-Aldrich (Buchs, Switzerland), doxycycline was from Clontech (Saint-Germain-en-Laye, France). Rapamycin was from LC Laboratories (Lucerna-Chem AG); trifluoperazine and carbamazepine were from Sigma-Aldrich; PD169316, PD98059, LY294002, and wortmannin were from Merck KGaA (Darmstadt, Germany); TGX-221 was from Cayman Chemical Company (Adipogen AG, Liestal, Switzerland); and SH-6 was purchased from Enzo Life Sciences (Lausen, Switzerland). Mouse SCF-secreting Chinese hamster ovary cells (CHO/SCF) were kindly provided by Dr Georg Häcker (University of Freiburg, Germany).

**Mice.** *Atg5<sup>fllox/fllox</sup>* mice<sup>14</sup> were kindly provided by Dr Christian Münz (University of Zurich, Switzerland). *Ly2z<sup>Cre/Cre</sup>* mice (B6.129P2-*Ly2z<sup>tm1(cre)flx</sup>*) were purchased from Jackson Laboratories (Bar Harbor, ME, USA) at backcross generation N6 and were further backcrossed to N10 with C57BL6/J mice.<sup>15</sup> *Atg5<sup>fllox/fllox</sup>* were crossed with *Ly2z<sup>Cre/Cre</sup>* mice to obtain *Atg5<sup>fllox/fllox</sup>-Ly2z<sup>Cre/Cre</sup>* (*Atg5<sup>NΔ</sup>*) mice. *Atg5<sup>fllox/fllox</sup>* mice were genotyped as described.<sup>14</sup> The animal studies were approved by Cantonal Veterinary Office of Bern, Switzerland.

**Sample collection from mouse bone marrow, blood, spleen, and lymph node.** All mice were analyzed between 8 and 12 weeks of age. Blood was collected from retro-orbital sinus of sedated mice, using heparinized disposable glass pipettes (Provet AG, Lyssach, Switzerland). Total leukocyte cell counts in blood were measured on a Scil Vet ABC hematology analyser (Horiba Medical, Montpellier, France). For serum preparation, the blood was left to clot for 2 h at room temperature and centrifuged (20 min, 3000 r.p.m., 4 °C).

Bone marrow cells were collected by flushing the femur with 5 ml of medium (100 U/ml penicillin/100  $\mu$ g/ml streptomycin, 1% FCS in PBS), using a 26-gauge needle, and filtering through a sterile 70- $\mu$ m nylon cell strainer. Spleen samples were pressed through a sterile 70- $\mu$ m nylon cell strainer with 5 ml of medium and erythrocytes were lysed for 10 min by adding nine parts of lysis buffer (0.16 M NH<sub>4</sub>Cl, 0.01 M KHCO<sub>3</sub>, 0.12 mM EDTA). Brachial and axillary lymph nodes were pressed through a sterile 70- $\mu$ m nylon cell strainer with 2 ml of medium. Bone marrow, spleen, and lymph-node single-cell suspensions were then washed with medium and the cells counted with hemocytometer, using the Türk's staining solution (Dr Grogg Chemie AG, Stettlen, Switzerland).

Primary bone marrow neutrophils were isolated by the negative selection technique, using an EasySep Mouse Neutrophil Enrichment Kit (Stemcell Technologies, Grenoble, France). Neutrophil purity was always higher than 93% and was assessed by staining with the Hemacolor Set (Merck KGaA) followed by light microscopy analysis.

**Hoxb8 neutrophils.** SCF-dependent conditional Hoxb8-immortalized neutrophil progenitor lines from WT mice were generated as described.<sup>24,25</sup> Undifferentiated Hoxb8 neutrophil precursor cells were kept in culture medium (RPMI-1640, supplemented with 10% FCS, 50  $\mu$ M  $\beta$ -mercaptoethanol, 100 U/ml penicillin/100  $\mu$ g/ml streptomycin, 5% of CHO/SCF cell conditioned medium (as a source of murine SCF), 100 nM 4-OHT). To set up differentiation, cells were washed two times with PBS and resuspended in differentiation medium (RPMI-1640, supplemented with 10% FCS, 50  $\mu$ M  $\beta$ -mercaptoethanol, 100 U/ml penicillin/100  $\mu$ g/ml streptomycin, 5% of CHO/SCF cell conditioned medium) in the absence of 4-OHT.

**Flow cytometry and cell sorting.** Heparinized blood (30  $\mu$ l) was stained with fluorochrome-labeled monoclonal antibodies for cell-surface markers for 45 min on ice. After staining, erythrocytes were lysed for 10 min at room temperature (BD FACS Lysing Solution; BD Biosciences, San Jose, CA, USA), and cells were washed two times with washing buffer (1% FCS in PBS).

Single-cell suspensions from bone marrow, spleen, and lymph nodes, or Hoxb8 neutrophils ( $0.5\text{--}1 \times 10^6$ ) were washed with 1 ml of washing buffer, blocked in the blocking solution (10% FCS, with 1% normal rat serum and 1% mouse serum in PBS) and stained with fluorochrome-labeled monoclonal antibodies for cell-surface staining for 45 min on ice.

For Ki-67 detection, the surface staining was followed by permeabilization of the cell membrane (CytoFix/CytoPerm; BD Biosciences). Cells were washed two times, incubated with Ki-67 antibody (2.5  $\mu$ g/ml) or rabbit IgG isotype control (2.5  $\mu$ g/ml) for 1 h on ice, washed again, and then stained with the secondary PerCP-conjugated goat-anti-rabbit antibody for 40 min on ice (15  $\mu$ g/ml).

Flow cytometry was performed on BD FACSCalibur flow cytometer (BD, Heidelberg, Germany). Data were analyzed using the FloJo 7.6.5. software (Tree Star, Ashland, OR, USA).

Cell sorting of neutrophil precursors (CD45<sup>+</sup>CD11b<sup>+</sup>Ly6G<sup>+</sup>CD115<sup>+</sup>SSC<sup>high</sup>) and GFP-positive Hoxb8 neutrophil precursors was done on the BD FACSaria cell sorter (BD).

**EdU staining of cycling bone marrow cells and chase into the peripheral blood.** Briefly, 100  $\mu$ l of EdU (Invitrogen) at the final concentration of 2 mg/ml in PBS was injected intravenously in the retro-orbital plexus of anesthetized mice. Some mice were left untreated as controls. Blood was harvested at five different time points and total leukocyte counts were determined using Scil

Vet ABC hematology analyser. Whole blood was stained with fluorochrome-conjugated surface antibodies against CD45 and Ly6G. EdU-positive cells in CD45<sup>+</sup> Ly6G<sup>+</sup> population were then detected using the Click-iT EdU Imaging Kit (Invitrogen).

**Quantitative real-time reverse transcription-PCR.** Primary bone marrow-derived neutrophils, sorted neutrophil precursors, or Hoxb8 neutrophils were lysed with RNA Lysis buffer (Promega, Duebendorf, Switzerland) and stored at  $-80^{\circ}\text{C}$  until PCR analysis. RNA was isolated with the SV Total RNA Isolation System (Promega). In all, 300 ng of total RNA was used for cDNA synthesis at  $50^{\circ}\text{C}$  for 1 h with SuperScript III Reverse Transcriptase (Invitrogen). The reverse transcription was followed by quantitative real-time PCR with the iCycler iQ5 Multicolor Real-Time PCR Detection System (Bio-Rad Laboratories, Hercules, CA, USA), using the following mouse *Atg5* primers (forward: 5'-CAC ACC CCT GAA ATG GCA TTA TCC-3'; reverse: 5'-AGC CTC AAC CGC ATC CTT GG-3') and SYBR Green Supermix (Bio-Rad) for the detection of PCR products. The constitutively expressed housekeeping gene *S18* was used to normalize the expression of *Atg5*.

**Immunoblotting.** Cell lysates of primary bone marrow-derived neutrophils, sorted neutrophil precursors, or Hoxb8 neutrophils were prepared by lysing the cells with the lysis buffer containing 50 mM Tris pH 7.4, 150 mM NaCl, 10% glycerol, 1% Triton X-100, 2 mM EDTA, 10 mM sodium pyrophosphate, 50 mM sodium fluoride, 200  $\mu\text{M}$   $\text{Na}_3\text{VO}_4$  and 1 mM PMSF in  $\text{H}_2\text{O}$ . Shortly before use, a protease inhibitor cocktail (Sigma-Aldrich) was added to the lysis buffer. Cells were lysed for 25 min on ice, with frequent vortexing. After the lysis, supernatants were collected following high-speed centrifugation (10 min, 13 000 r.p.m.,  $4^{\circ}\text{C}$ ). In all, 50  $\mu\text{g}$  of protein was loaded on the 12% sodium dodecyl sulfate (SDS) polyacrylamide gel (Expedeon, Lucerna-Chem). The lysates were separated by electrophoresis under reducing conditions and transferred onto polyvinylidene difluoride (PVDF) membranes (Immobilon-P; Millipore, Carrigtwohill, Ireland). Membranes were blocked with 5% non-fat dry milk in Tris-buffered saline solution containing 0.1% Tween 20 (TBST) for 1 h and then incubated with primary antibodies (see *Antibodies*) in TBST and 5% non-fat dry milk at  $4^{\circ}\text{C}$  overnight. Membranes were washed using TBST and then incubated with the corresponding HRP-conjugated secondary antibodies and visualized by chemiluminescence (ECL Western Blotting Analysis System; GE Healthcare or Luminata Forte; Millipore Corporation, Billerica, MA, USA).

**Detecting autophagosome formation by Autodot staining.** Primary bone marrow-derived neutrophils were incubated on a coverslip in a 24-well plate (1 h,  $37^{\circ}\text{C}$ , 5%  $\text{CO}_2$ ) at the concentration of  $3 \times 10^6$  cells/ml in 100  $\mu\text{l}$  of RPMI-1640 medium, supplemented with 10% FCS. The cells were left untreated or stimulated with 100 nM rapamycin for 1 h. After the incubation, the medium was gently removed from the coverslip and the cells were stained with 100  $\mu\text{l}$  of AUTODot Autophagy Visualization Dye (0.15 mM monodansylpentane in PBS; Abgent) at  $33^{\circ}\text{C}$  for 15 min. The dye was gently removed and the cells were fixed with 4% paraformaldehyde solution for 5 min at room temperature, washed three times with 500  $\mu\text{l}$  of PBS, mounted on a microscope slide with 3  $\mu\text{l}$  mounting medium (Dako, Baar, Switzerland) and stored at  $4^{\circ}\text{C}$  overnight, protected from light. The slides were analyzed the next day by confocal laser scanning microscopy (Carl Zeiss AG, Jena, Germany) equipped with argon, blue diode, and helium-neon lasers. The intensity of the staining was analyzed by the ImageJ software (<http://rsb.info.nih.gov/ij/>) and calculated as the mean maximum fluorescence intensity of a cell. A hundred cells per condition were analyzed.

**Lentiviral gene transfer.** In all,  $0.5 \times 10^6$  Hoxb8 neutrophil precursors were resuspended in 500  $\mu\text{l}$  of culture medium and transduced with custom mouse shRNA *Atg5* lentiviral construct: pRSI-U6Tet-shm.*Atg5\_cust-UbiC-TetR-2A-TagGFP2-W* (Cellesta, Mountain View, CA, USA) with the target sequence GCAGAACCATACTATTGCTT, at the multiplicity of infection of 40. Control cells were transduced with an empty lentiviral construct: pRSI-U6Tet-sh-UbiC-TetR-2A-TagGFP2-W. After spin infection (1 h, 1500 r.p.m.,  $30^{\circ}\text{C}$ ) in the presence of polybrene (5  $\mu\text{g}/\text{ml}$ ), 1.5 ml of fresh culture medium was added to the cells. Three to five days after infection, the cells were sorted for GFP-positive population. Before setting up the differentiation, the expression of shRNA was induced by doxycycline treatment (100 ng/ml, 24 h). During differentiation, the doxycycline-containing medium was refreshed every 48 h.

Mouse *Atg5* (Gene ID: 158508499, NM\_053069) was sub-cloned in pRRL-cPPT-hPGK-mcs-WPRE vector with addition of GFP under ubiquitin promoter obtained

from Dr Didier Trono (EPFL, Lausanne, Switzerland), using forward primer for mouse *Atg5*, containing a PmeI restriction site: 5'-GCG CGT TTA AAC ATG ACA GAT GAC AAA GAT GTG CTT CGA G-3' and reverse primer, containing a *NheI* restriction site: 5'-GCG CGC TAG CTC AAT CTG TTG GCT GGG GGA CA-3'. Recombinant virus constructs were produced by calcium phosphate transfection together with the envelope vector PMD2.G and the packaging vectors psPAX2 for lentivirus (all provided by Dr Trono) into 293T cells. For virus stocks, the supernatant was collected 24, 48, and 72 h after transfection and cleared by passing through sterile 0.45  $\mu\text{m}$  pore size filter and 10x concentrated at  $4^{\circ}\text{C}$  in a Beckman Coulter ultracentrifuge (Palo Alto, CA, USA) with the SW41-Ti rotor (90 min, 55 000 g). Pellets were resuspended in RPMI-1640, supplemented with 10% FCS, and aliquoted and stored at  $-80^{\circ}\text{C}$ . In all,  $0.5 \times 10^6$  Hoxb8 neutrophil precursors were resuspended in 500  $\mu\text{l}$  of culture medium and transduced with the *Atg5* lentivirus or the empty vector, at a multiplicity of infection of 25. After spin infection (1 h, 1500 r.p.m.,  $30^{\circ}\text{C}$ ) in the presence of polybrene (1  $\mu\text{g}/\text{ml}$ ), 1.5 ml of fresh culture medium was added to the cells. Two to three days after infection, the cells were sorted for GFP-positive population.

**Pharmacological treatment of Hoxb8 neutrophils.** Carbamazepine (10  $\mu\text{M}$ ), LY294002 (500 nM), PD169316 (1  $\mu\text{M}$ ), PD98059 (1  $\mu\text{M}$ ), rapamycin (100 nM), SH-6 (5  $\mu\text{M}$ ), TGX-221 (50 nM), trifluoperazine (500 nM), and wortmannin (30 nM) were added to the differentiation medium at the beginning of Hoxb8 neutrophil differentiation. At the indicated concentrations, none of the drugs induced cell death.

**Histology.** Spleens were harvested from WT and *Atg5*<sup>NΔ</sup> mice, perfused with PBS, fixed in 4% paraformaldehyde for 24 h, and embedded in paraffin blocks. Histological transverse 4- $\mu\text{m}$  sections of the spleen were deparaffinized, rehydrated, and stained with Naphtol AS-D Chloroacetate solution according to the instructions of the manufacturer (Naphtol AS-D Chloroacetate (Specific Esterase) Kit; Sigma-Aldrich).

**G-CSF and GM-CSF immunoassays.** The serum from WT and *Atg5*<sup>NΔ</sup> mice was diluted 1 : 2 with Sample diluent (Bio-Rad) and pipetted into a 96-well plate. The magnetic bead-based immunoassay was carried out according to the instructions of the manufacturer (Bio-Plex Pro Mouse Cytokine Assay; Bio-Rad) and the read-out was performed on the Bio-Plex MAGPIX Multiplex Reader (Bio-Rad).

**Degranulation assays.** Primary bone marrow-derived neutrophils from WT and *Atg5*<sup>NΔ</sup> mice were resuspended in RPMI-1640 at  $10 \times 10^6$  cells/ml and left to settle for 20 min. They were then pretreated with cytochalasin B (Sigma-Aldrich; 5  $\mu\text{g}/\text{ml}$ ; 5 min) and stimulated with Formyl-Methionyl-Leucyl-Phenylalanine (Sigma-Aldrich; 1  $\mu\text{M}$ ; 1 h). The supernatants were acquired following the centrifugation step (20 min, 2000 r.p.m.,  $4^{\circ}\text{C}$ ), aliquoted into three parts, and stored at  $-80^{\circ}\text{C}$  until analysis. The granule content was determined by enzyme-linked immunosorbent assays (ELISAs) according to the instructions of the manufacturer. Cathepsin G ELISA Kit was from Qayee Biotechnology (Shanghai, China), lactoferrin ELISA Kit was from Blue Gene (Shanghai, China) and MMP-9 ELISA Kit was from USCN Life Science Inc. (Wuhan, China).

**Cell death assays.** Whole blood from WT and *Atg5*<sup>NΔ</sup> mice was acquired into the heparin-coated blood collecting system (Sartedt, Nümbrecht, Germany) and incubated at  $37^{\circ}\text{C}$ , gently shaking, for 48 h. In all, 30  $\mu\text{l}$  of blood was collected at different time points and erythrocytes were lysed by adding nine parts of lysis buffer (0.16 M  $\text{NH}_4\text{Cl}$ , 0.01 M  $\text{KHCO}_3$ , 0.12 mM EDTA). Following two washing steps (1% FCS in PBS), the cells were stained with anti-Ly6G antibody. Immediately before measurement, propidium iodide (Sigma-Aldrich) was added to stained blood samples at 10  $\mu\text{g}/\text{ml}$  and viability was measured by flow cytometry.

Primary bone marrow-derived neutrophils from WT and *Atg5*<sup>NΔ</sup> mice were cultured at  $1 \times 10^6$  cells/ml for the indicated times in the absence or presence of a broad spectrum caspase inhibitor Q-VD-OPH (10  $\mu\text{M}$ ), G-CSF (25 ng/ml; Peprotech, London, UK), GM-CSF (10 ng/ml; R&D Systems, Abingdon, UK), IL-3 (1  $\mu\text{g}/\text{ml}$ ; BD Biosciences), IL-5 (25 ng/ml; R&D Systems), anti-CD95 antibody (1  $\mu\text{g}/\text{ml}$ ; MBL International Corp., Woburn, MA, USA), TNF- $\alpha$  (10 ng/ml; R&D Systems), LPS (100 ng/ml; Sigma-Aldrich) and C5a (10 ng/ml; Hycult Biotech, Uden, The Netherlands) in complete culture medium (RPMI-1640, supplemented with 10% FCS, 100 U/ml penicillin/100  $\mu\text{g}/\text{ml}$  streptomycin). Immediately before measurement, propidium iodide was added to cell suspension at 10  $\mu\text{g}/\text{ml}$  and viability was measured by flow cytometry (BD FACSCalibur).

**In vivo neutrophil recruitment.** In all, 350 ng IL-8 (R&D Systems) in 1 ml PBS was injected in the peritoneal cavity of anesthetized mice. Some mice were treated with PBS alone and used as negative controls. After 4 h, the peritoneal cavity was washed twice with 5 ml of PBS, and both fractions pooled together. Total cell counts in peritoneal exudate were counted by hemocytometer, using the Türk's staining solution. The percentage of neutrophils in the peritoneal exudate cells was determined by flow cytometry, whereby gating was done on the CD45<sup>+</sup>CD11b<sup>+</sup>Ly6G<sup>+</sup> population (Supplementary Figure S2). The percentages were confirmed by a second method, staining with the Hematocolor Set and light microscopic analysis.

**Phagocytosis assay.** Fluoresbrite Polychromatic Red Microspheres (Polysciences, Inc., Warrington, PA, USA) were diluted with RPMI-1640 to attain the working concentration ( $2.5 \times 10^8$  particles/ml). In all, 140  $\mu$ l of working suspension was opsonized with 35  $\mu$ l of mouse serum for 30 min (180 r.p.m., 37 °C). Hoxb8 neutrophils and primary bone marrow-derived neutrophils ( $0.1 \times 10^6$ ) were resuspended in 100  $\mu$ l of RPMI-1640 medium, supplemented with 10% FCS and 25  $\mu$ l of opsonized beads was then added to the cells. Simultaneously, 25  $\mu$ l of non-opsonized beads was added to the second sample of cells and served as a negative control. The cells were incubated with the beads for 1 h (130 r.p.m., 37 °C). Phagocytosis was stopped by adding 200  $\mu$ l of ice-cold PBS with 0.02% EDTA to the cells. After one washing step with 400  $\mu$ l of ice-cold PBS, the cells were analyzed by flow cytometry (BD FACSCalibur).

**ROS production assay.** In total,  $0.25 \times 10^6$  Hoxb8 neutrophils and primary bone marrow-derived neutrophils were resuspended in 200  $\mu$ l of X-Vivo serum-free medium (Lonza, Verviers, Belgium). Cells were left untreated (negative control) or primed with GM-CSF (50 ng/ml; 20 min) and then stimulated with C5a (100 nM; 15 min). Simultaneously with C5a, dihydrorhodamine (Sigma-Aldrich) at the final concentration of 1  $\mu$ M was added to the cells. ROS production was stopped by adding 200  $\mu$ l of ice-cold PBS. Dihydrorhodamine oxidation was measured by flow cytometry (BD FACSCalibur).

**Bacterial killing assay.** Single colonies of *Escherichia (E.) coli GFP M 91655* were cultured in Luria broth base (LB) medium (Sigma) at 37 °C, shaking at 220 r.p.m. overnight. Bacterial cultures were diluted 1 : 100 in LB medium, then grown to mid-logarithmic growth phase ( $OD_{600} = 0.7$ ) and centrifuged at 1000x g for 5 min. Bacterial pellets were washed twice in 1 x Hank's Balanced Salt Solution (HBSS; LuBioScience GmbH) and gently spun at 100 xg for 5 min to remove any clumped bacteria. Bacteria were opsonized with 10% mouse sera (heat-inactivated) in 1 x HBSS, rotating end-over-end (6 r.p.m.) for 20 min at 37 °C, and then used immediately. The bacterial killing assay was performed as previously described.<sup>68</sup> Briefly, primary bone marrow-derived neutrophils from WT and *Atg5<sup>fl/fl</sup>* mice ( $1 \times 10^7$ /ml) were resuspended in 200  $\mu$ l of RPMI-1640 medium, supplemented with 2% FCS. In all, 20  $\mu$ l of normal mouse sera was added to the neutrophils, followed by the addition of 220  $\mu$ l of the opsonized bacteria. Neutrophils were then co-cultured with opsonized bacteria in a total volume of 440  $\mu$ l (1 : 1 ratio), rotating end-over-end (6 r.p.m.) for 45 min at 37 °C. At the end of the incubation period, 440  $\mu$ l ice-cold 1 x HBSS was added to each tube to stop the reaction, and the tubes were centrifuged gently using a swing-out rotor (5 min, 100 xg, 4 °C). Supernatants were collected, diluted 1 : 200, plated on agar, and grown overnight before counting the colonies. Tubes containing bacteria alone were treated the same way and used as controls.

**Statistical analysis.** Analysis of all data was performed by the Prism software (GraphPad Software Inc., San Diego, CA, USA). All data were expressed as mean  $\pm$  S.E.M. Results were analyzed using unpaired Student's *t*-test or two-way ANOVA with Bonferroni's *post-hoc* test, with *P* < 0.05 considered as statistically significant.

## Conflict of Interest

The authors declare no conflict of interest.

**Acknowledgements.** This study was funded by the Swiss National Science Foundation (Grant number 310030\_146181 to HUS). CB is funded by the Swiss National Science Foundation (Grant number 310030\_149790). We thank Dr M Baumann for technical support during the flow-cytometric analyses of blood

and bone marrow cells from *Atg5<sup>fl/fl</sup>* mice and Dr Elena Federzoni for the generation of *ATG5*-overexpressing Hoxb8 neutrophils.

- Boya P, Reggiori F, Codogno P. Emerging regulation and functions of autophagy. *Nat Cell Biol* 2013; **15**: 713–720.
- Mizushima N, Noda T, Ohsumi Y. Apg16p is required for the function of the Apg12p-Apg5p conjugate in the yeast autophagy pathway. *EMBO J* 1999; **18**: 3888–3896.
- Mizushima N, Yamamoto A, Hatano M, Kobayashi Y, Kabeya Y, Suzuki K et al. Dissection of autophagosome formation using Apg5-deficient mouse embryonic stem cells. *J Cell Biol* 2001; **152**: 657–668.
- Kabeya Y, Mizushima N, Ueno T, Yamamoto A, Kirisako T, Noda T et al. LC3, a mammalian homologue of yeast Apg8p, is localized in autophagosomal membranes after processing. *EMBO J* 2000; **19**: 5720–5728.
- Bjorkoy G, Lamark T, Brech A, Outzen H, Perander M, Overvatn A et al. p62/SQSTM1 forms protein aggregates degraded by autophagy and has a protective effect on huntingtin-induced cell death. *J Cell Biol* 2005; **171**: 603–614.
- Stephenson LM, Miller BC, Ng A, Eisenberg J, Zhao Z, Cadwell K et al. Identification of Atg5-dependent transcriptional changes and increases in mitochondrial mass in Atg5-deficient T lymphocytes. *Autophagy* 2009; **5**: 625–635.
- Pua HH, Dzhagalov I, Chuck M, Mizushima N, He YW. A critical role for the autophagy gene Atg5 in T cell survival and proliferation. *J Exp Med* 2007; **204**: 25–31.
- Miller BC, Zhao Z, Stephenson LM, Cadwell K, Pua HH, Lee HK et al. The autophagy gene Atg5 plays an essential role in B lymphocyte development. *Autophagy* 2008; **4**: 309–314.
- Zhang Y, Morgan MJ, Chen K, Choksi S, Liu ZG. Induction of autophagy is essential for monocytes-macrophage differentiation. *Blood* 2012; **119**: 2895–2905.
- Lee HK, Mattei LM, Steinberg BE, Alberts P, Lee YH, Chervonsky A et al. In vivo requirement for Atg5 in antigen presentation by dendritic cells. *Immunity* 2010; **32**: 227–239.
- Kundu M, Lindsten T, Yang CY, Wu J, Zhao F, Zhang J et al. Ulk1 plays a critical role in the autophagic clearance of mitochondria and ribosomes during reticulocyte maturation. *Blood* 2008; **112**: 1493–1502.
- Mortensen M, Ferguson DJ, Edelmann M, Kessler B, Morten KJ, Komatsu M et al. Loss of autophagy in erythroid cells leads to defective removal of mitochondria and severe anemia in vivo. *Proc Natl Acad Sci USA* 2010; **107**: 832–837.
- Kuma A, Hatano M, Matsui M, Yamamoto A, Nakaya H, Yoshimori T et al. The role of autophagy during the early neonatal starvation period. *Nature* 2004; **432**: 1032–1036.
- Hara T, Nakamura K, Matsui M, Yamamoto A, Nakahara Y, Suzuki-Migishima R et al. Suppression of basal autophagy in neural cells causes neurodegenerative disease in mice. *Nature* 2006; **441**: 885–889.
- Clausen BE, Burkhardt C, Reith W, Renkawitz R, Forster I. Conditional gene targeting in macrophages and granulocytes using LysMCre mice. *Transgenic Res* 1999; **8**: 265–277.
- Zhao Z, Fux B, Goodwin M, Dunay IR, Strong D, Miller BC et al. Autophagosome-independent essential function for the autophagy protein Atg5 in cellular immunity to intracellular pathogens. *Cell Host Microbe* 2008; **4**: 458–469.
- Demetri GD, Griffin JD. Granulocyte colony-stimulating factor and its receptor. *Blood* 1991; **78**: 2791–2808.
- Richards MK, Liu F, Iwasaki H, Akashi K, Link DC. Pivotal role of granulocyte colony-stimulating factor in the development of progenitors in the common myeloid pathway. *Blood* 2003; **102**: 3562–3568.
- Metcalfe D, Begley CG, Williamson DJ, Nice EC, De Lamerter J, Mermoud JJ et al. Hemopoietic responses in mice injected with purified recombinant murine GM-CSF. *Exp Hematol* 1987; **15**: 1–9.
- Gerdes J, Lemke H, Baisch H, Wacker HH, Schwab U, Stein H. Cell cycle analysis of a cell proliferation-associated human nuclear antigen defined by the monoclonal antibody Ki-67. *J Immunol* 1984; **133**: 1710–1715.
- Bainton DF, Ulliyot JL, Farquhar MG. The development of neutrophilic polymorphonuclear leukocytes in human bone marrow. *J Exp Med* 1971; **134**: 907–934.
- Klausen P, Bjerregaard MD, Borregaard N, Cowland JB. End-stage differentiation of neutrophil granulocytes in vivo is accompanied by up-regulation of p27kip1 and down-regulation of CDK2, CDK4, and CDK6. *J Leukoc Biol* 2004; **75**: 569–578.
- Salic A, Mitchison TJ. A chemical method for fast and sensitive detection of DNA synthesis in vivo. *Proc Natl Acad Sci USA* 2008; **105**: 2415–2420.
- Wang GG, Calvo KR, Pasillas MP, Sykes DB, Hacker H, Kamps MP. Quantitative production of macrophages or neutrophils ex vivo using conditional Hoxb8. *Nat Methods* 2006; **3**: 287–293.
- Guizeler U, Rabachini T, Dahinden CA, Salamanidis M, Brumatti G, Eckert PG et al. In vitro differentiation of near-unlimited numbers of functional mouse basophils using conditional Hoxb8. *Allergy* 2013; **68**: 604–613.
- Borregaard N, Cowland JB. Granules of the human neutrophilic polymorphonuclear leukocyte. *Blood* 1997; **89**: 3503–3521.
- Noda T, Ohsumi Y. Tor, a phosphatidylinositol kinase homologue, controls autophagy in yeast. *J Biol Chem* 1998; **273**: 3963–3966.
- Jung CH, Ro SH, Cao J, Otto NM, Kim DH. mTOR regulation of autophagy. *FEBS Lett* 2010; **584**: 1287–1295.
- Blommaert EFC, Luiken JJFP, Blommaert PJE, van Woerkom GM, Meijer AJ. Phosphorylation of ribosomal protein S6 is inhibitory for autophagy in isolated rat hepatocytes. *J Biol Chem* 1995; **270**: 2320–2326.



30. Klionsky DJ, Emr SD. Autophagy as a regulated pathway of cellular degradation. *Science* 2000; **290**: 1717–1721.
31. Sarkar S, Floto RA, Berger Z, Imarisio S, Cordenier A, Pasco M *et al*. Lithium induces autophagy by inhibiting inositol monophosphatase. *J Cell Biol* 2005; **170**: 1101–1111.
32. Zhang L, Yu J, Pan H, Hu P, Hao Y, Cai W *et al*. Small molecule regulators of autophagy identified by an image-based high-throughput screen. *Proc Natl Acad Sci USA* 2007; **104**: 19023–19028.
33. Renna M, Jimenez-Sanchez M, Sarkar S, Rubinsztein DC. Chemical inducers of autophagy that enhance the clearance of mutant proteins in neurodegenerative diseases. *J Biol Chem* 2010; **285**: 11061–11067.
34. Inoki K, Li Y, Zhu T, Wu J, Guan KL. TSC2 is phosphorylated and inhibited by Akt and suppresses mTOR signalling. *Nat Cell Biol* 2002; **4**: 648–657.
35. Yang Z, Klionsky DJ. Mammalian autophagy: core molecular machinery and signaling regulation. *Curr Opin Cell Biol* 2010; **22**: 124–131.
36. Li Y, Inoki K, Vacratis P, Guan KL. The p38 and MK2 kinase cascade phosphorylates tuberlin, the tuberous sclerosis 2 gene product, and enhances its interaction with 14-3-3. *J Biol Chem* 2003; **278**: 13663–13671.
37. Yousefi S, Simon HU. Autophagy in cells of the blood. *Biochim Biophys Acta* 2009; **1793**: 1461–1464.
38. Betin VM, Singleton BK, Parsons SF, Anstee DJ, Lane JD. Autophagy facilitates organelle clearance during differentiation of human erythroblasts: evidence for a role for ATG4 paralogs during autophagosome maturation. *Autophagy* 2013; **9**: 881–893.
39. Conway KL, Kuballa P, Khor B, Zhang M, Shi HN, Virgin HW *et al*. ATG5 regulates plasma cell differentiation. *Autophagy* 2013; **9**: 528–537.
40. Jacquet A, Obba S, Boyer L, Dufies M, Robert G, Gounon P *et al*. Autophagy is required for CSF-1-induced macrophagic differentiation and acquisition of phagocytic functions. *Blood* 2012; **119**: 4527–4531.
41. Colosetti P, Puissant A, Robert G, Luciano F, Jacquet A, Gounon P *et al*. Autophagy is an important event for megakaryocytic differentiation of the chronic myelogenous leukemia K562 cell line. *Autophagy* 2009; **5**: 1092–1098.
42. Liu F, Lee JY, Wei H, Tanabe O, Engel JD, Morrison SJ *et al*. FIP200 is required for the cell-autonomous maintenance of fetal hematopoietic stem cells. *Blood* 2010; **116**: 4806–4814.
43. Mortensen M, Soilleux EJ, Djordjevic G, Tripp R, Lutteropp M, Sadighi-Akha E *et al*. The autophagy protein Atg7 is essential for hematopoietic stem cell maintenance. *J Exp Med* 2011; **208**: 455–467.
44. Salemi S, Yousefi S, Constantinescu MA, Fey MF, Simon HU. Autophagy is required for self-renewal and differentiation of adult human stem cells. *Cell Res* 2012; **22**: 432–435.
45. Singh R, Xiang Y, Wang Y, Baikati K, Cuervo AM, Luu YK *et al*. Autophagy regulates adipose mass and differentiation in mice. *J Clin Invest* 2009; **119**: 3329–3339.
46. Zhang Y, Goldman S, Baerga R, Zhao Y, Komatsu M, Jin S. Adipose-specific deletion of autophagy-related gene 7 (*atg7*) in mice reveals a role in adipogenesis. *Proc Natl Acad Sci USA* 2009; **106**: 19860–19865.
47. Baerga R, Zhang Y, Chen PH, Goldman S, Jin S. Targeted deletion of autophagy-related 5 (*atg5*) impairs adipogenesis in a cellular model and in mice. *Autophagy* 2009; **5**: 1118–1130.
48. Liu F, Fang F, Yuan H, Yang D, Chen Y, Williams L *et al*. Suppression of autophagy by FIP200 deletion leads to osteopenia in mice through the inhibition of osteoblast terminal differentiation. *J Bone Miner Res* 2013; **28**: 2414–2430.
49. Komatsu M, Waguri S, Chiba T, Murata S, Iwata J, Tanida I *et al*. Loss of autophagy in the central nervous system causes neurodegeneration in mice. *Nature* 2006; **441**: 880–884.
50. Humbert M, Mueller C, Fey MF, Tschan MP. Inhibition of damage-regulated autophagy modulator-1 (DRAM-1) impairs neutrophil differentiation of NB4 APL cells. *Leuk Res* 2012; **36**: 1552–1556.
51. Xie N, Zhong L, Liu L, Fang Y, Qi X, Cao J *et al*. Autophagy contributes to dasatinib-induced myeloid differentiation of human acute myeloid leukemia cells. *Biochem Pharmacol* 2014; **89**: 74–85.
52. Wang Z, Cao L, Kang R, Yang M, Liu L, Zhao Y *et al*. Autophagy regulates myeloid cell differentiation by p62/SQSTM1-mediated degradation of PML-RAR $\alpha$  oncoprotein. *Autophagy* 2011; **7**: 401–411.
53. Yan ZW, Hou JK, He W, Fan L, Huang Y. Chloroquine enhances cobalt chloride-induced leukemic cell differentiation via the suppression of autophagy at the late phase. *Biochem Biophys Res Commun* 2013; **430**: 926–932.
54. Liu G, Hu X, Sun B, Yang T, Shi J, Zhang L *et al*. Phosphatase Wip1 negatively regulates neutrophil development through p38 MAPK-STAT1. *Blood* 2013; **121**: 519–529.
55. Funakoshi T, Latif A, Galsky MD. Risk of hematologic toxicities in patients with solid tumors treated with everolimus: a systematic review and meta-analysis. *Crit Rev Oncol Hematol* 2013; **88**: 30–41.
56. Liu H, He Z, von Rütte T, Yousefi S, Hunger RE, Simon HU. Down-regulation of autophagy-related protein 5 (ATG5) contributes to the pathogenesis of early-stage cutaneous melanoma. *Sci Transl Med* 2013; **5**: 202ra123.
57. Gурpinar E, Grizzle WE, Shacka JJ, Mader BJ, Li N, Piazza NA *et al*. A novel sulindac derivative inhibits lung adenocarcinoma cell growth through suppression of Akt/mTOR signaling and induction of autophagy. *Mol Cancer Ther* 2013; **12**: 663–674.
58. Chen K, Shou LM, Lin F, Duan WM, Wu MY, Xie X *et al*. Artesunate induces G2/M cell cycle arrest through autophagy induction in breast cancer cells. *Anticancer Drugs* 2014; **25**: 652–662.
59. Narita M, Young AR, Narita M. Autophagy facilitates oncogene-induced senescence. *Autophagy* 2009; **5**: 1046–1047.
60. Xu Y, Li N, Xiang R, Sun P. Emerging roles of the p38 MAPK and PI3K/AKT/mTOR pathways in oncogene-induced senescence. *Trends Biochem Sci* 2014; **39**: 268–276.
61. Lee IH, Kawai Y, Fergusson MM, Rovira II, Bishop AJ, Motoyama N *et al*. Atg7 modulates p53 activity to regulate cell cycle and survival during metabolic stress. *Science* 2012; **336**: 225–228.
62. Courtois-Cox S, Genthner Williams SM, Reczek EE, Johnson BW, McGillicuddy LT, Johannessen CM *et al*. A negative feedback signaling network underlies oncogene-induced senescence. *Cancer Cell* 2006; **10**: 459–472.
63. Belaid A, Cerezo M, Chargui A, Corcelle-Termeau E, Pedetour F, Giuliano S *et al*. Autophagy plays a critical role in the degradation of active RHOA, the control of cell cytokinesis, and genomic stability. *Cancer Res* 2013; **73**: 4311–4322.
64. Maskey D, Yousefi S, Schmid I, Zlobec I, Perren A, Friis R *et al*. ATG5 is induced by DNA-damaging agents and promotes mitotic catastrophe independent of autophagy. *Nat Commun* 2013; **4**: 2130.
65. Simon HU, Yousefi S, Schmid I, Friis R. ATG5 can regulate p53 expression and activation. *Cell Death Dis* 2014; **5**: e1339.
66. Yang A, Walker N, Bronson R, Kaghad M, Oosterwegel M, Bonnin J *et al*. p73-deficient mice have neurological, pheromonal and inflammatory defects but lack spontaneous tumours. *Nature* 2000; **404**: 99–103.
67. He Z, Liu H, Agostini M, Yousefi S, Perren A, Tschan MP *et al*. p73 regulates autophagy and hepatocellular lipid metabolism through a transcriptional activation of the ATG5 gene. *Cell Death Differ* 2013; **20**: 1415–1424.
68. Morshed M, Yousefi S, Stöckle C, Simon HU, Simon D. Thymic stromal lymphopoietin stimulates the formation of eosinophil extracellular traps. *Allergy* 2012; **67**: 1127–1137.

Supplementary Information accompanies this paper on Cell Death and Differentiation website (<http://www.nature.com/cdd>)